Rare Metal Materials and Engineering
Volume 51, Issue 9, September 2022
Available online at www.rmme.ac.cn

Science Press

Cite this article as: Wu Xiaoyan, Luo Wei, Jiang Haitao. Effect of Probe Length on Microstructure and Mechanical Properties of Friction Stir Lap-Welded Aluminum Alloy and Steel[J]. Rare Metal Materials and Engineering, 2022, 51(09): 3197-3203.

ARTICLE

Effect of Probe Length on Microstructure and Mechanical Properties of Friction Stir Lap-Welded Aluminum Alloy and Steel

Wu Xiaoyan, Luo Wei, Jiang Haitao

National Engineering Research Center for Advanced Rolling and Intelligent Manufacturing, University of Science and Technology Beijing, Beijing 100083, China

Abstract: The 6061 aluminum alloy and QP980 steel were lap-welded by friction stir welding (FSW) technique, and the effect of different probe lengths of 1.5 and 2.1 mm on the microstructures and properties of welded joints was investigated. Results show that the FSW lap-welded joints of 6061 aluminum alloy/QP980 steel consist of three layers: the upper layer is aluminum alloy, the middle layer is composed of Fe, Al, and intermetallic compounds, and the under layer is steel. When the probe length is 2.1 mm, the aluminum layer contains scattered steel fragments. Two kinds of intermetallic compounds can be detected: the dark gray layer close to Al is Fe_4Al_{13} phase, and the one close to steel is Fe_2Al_5 phase. With extending the probe length, the fracture load of the joints is decreased from 4 kN to 3 kN. The joints welded by short probe fracture at the bonding interface, whereas those welded by long probe fracture at the mixture zone of Al and steel. The fracture position change is caused by the porosities and steel fragments. In addition, the steel fragments embedded in the Al matrix promote the stress concentration and crack initiation during the deformation process, therefore decreasing the mechanical properties of the joints.

Key words: friction stir lap-welding; probe length; intermetallic compounds; fracture load

Aluminum alloys and ultra-high strength steels are commonly used jointly in automobile industry due to their excellent properties, controllable flexibility, and low cost[1,2]. Fusion welding techniques, such as argon-arc welding, laser welding, and electric resistance welding, have been widely used to join dissimilar materials. However, the differences in thermophysical characteristics and crystal structures of Al and Fe are too large to obtain welds by fusion welding technique. In addition, the brittle intermetallic compounds (IMCs), such as Fe_3Al and FeAl phases, can decrease the mechanical properties of welding structures[3]. Thus, the combination of Al and steel is restricted due to the disadvantages of fusion welding in the vehicle fields[4].

Friction stir welding (FSW) is a solid joining process with great industrial potential[5], which is characterized by the relatively small heat input and less formation of concomitant IMCs layer[6,7]. There is no bulk melting of the parent material in the joint during FSW process, so the joints do not suffer from pores or hot cracking. Therefore, FSW has been widely applied to aluminum alloys and steels[8,9]. During FSW process, the materials undergo very large strains at high temperatures under a relatively high strain rate. Thus, FSW normally involves complex interactions and components, because of mass and heat transports, plastic deformation, fracture damage, and microstructure evolution[10-13]. Consequently, the material microstructure and mechanical properties in the welded region are highly complex.

The effects of process parameters, including rotation speed, welding speed, and tool offset, on the joint microstructure evolution and mechanical properties have been studied[14,15]. Pourali et al[16] reported that the optimum tensile strength of 1100Al/low carbon steel joint is achieved after lap-welding at low welding temperature and high rotation speed. Zhao et al[17] investigated the effects of tool size and tool offset on AA6061/

Received date: September 23, 2021
Foundation item: Fundamental Research Funds for the Central Universities (FRF-TP-19-083A1)
Corresponding author: Jiang Haitao, Ph. D., Professor, National Engineering Research Center for Advanced Rolling and Intelligent Manufacturing, University of Science and Technology Beijing, Beijing 100083, P. R. China, Tel: 0086-10-62332598, E-mail: jianght@ustb.edu.cn

transformation-induced plasticity steel after FSW and proved that the tool parameters can determine the amount of generated heat and the thickness of IMC layer. Dehghani et al[18] also studied the effect of FSW parameters on IMCs and defect formation in Al/mild steel joints. Various IMCs, including FeAl, Fe_4Al_{13} ($FeAl_3$), Fe_2Al_5, and $FeAl_{14}$, can be found in the Al/steel joint after FSW[19,20]. As for the friction stir lap welding, the probe length definitely affects the microstructure and mechanical properties of the joints. Chen et al[21] discussed the effect of probe length on microstructure and mechanical properties of friction stir lap-welded Mg/steel joints. The microstructure at the bonding interface, the fracture loads, and the fracture locations of the joints are changed significantly with different probe lengths. However, the effect of probe length on the microstructure evolution and mechanical properties of Al/steel joint is rarely reported.

In this research, 6061 Al alloy and QP980 steel were welded by FSW with two different probe lengths. The microstructure evolution and mechanical properties of joints along the bonding interface were investigated, providing a guidance for the microstructure control in the fabrication of FSW joints.

1 Experiment

The base materials used in this study were 6061 aluminum alloy plates with 2 mm in thickness and QP980 high strength steel plates with 1.5 mm in thickness. The chemical composition of 6061Al and QP980 steel is shown in Table 1 and Table 2, respectively. The rectangular specimens of these two alloys with dimension of 150 mm×100 mm were lap-welded by FSW, as shown in Fig. 1a. Before welding, the surfaces of the plates were ground and wiped using sandpaper and acetone to remove the surface oxides and oil contaminations, respectively. FSW was conducted with a tool of 15 mm in diameter and probes of different lengths. Two probes with length of 1.5 and 2.1 mm were used in this research, which were denoted as short probe and long probe, respectively, as shown in Fig.1b. The short probe and the long one could be inserted only in aluminum alloy and in aluminum alloy with steel, respectively. The tool rotation rate and transverse speed were 1000 r/min and 120 mm·min^{-1}, respectively.

After welding, a wire-electrode cutting machine was used to prepare the specimens for metallographic observation and tensile tests. The laser confocal microscope LEXT OLS4100

Table 1 Chemical composition of 6061Al base materials (wt%)

Mg	Si	Fe	Cu	Mn	Zn	Ti	Al
1.14	0.57	0.62	0.21	0.15	0.25	0.15	Bal.

Table 2 Chemical composition of QP980 steel base materials (wt%)

C	Si	Mn	P	S	Al	Fe
0.20	1.30	2.00	0.013	0.008	0.04	Bal.

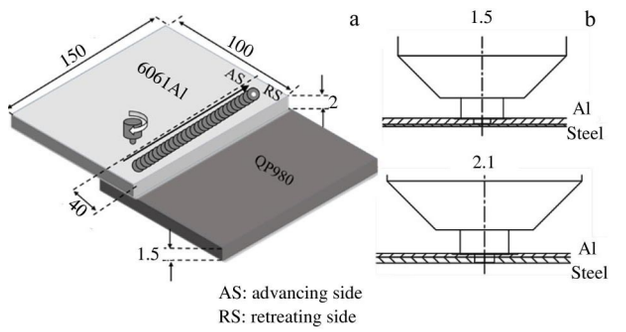

Fig.1 Schematic diagrams of FSW process (a) and welding probes with different lengths (b)

was employed to characterize the microstructure of the joints. The mechanically polished specimen was analyzed by electron backscattered diffraction (EBSD). The specimen was rectangular and its gage length was 25 mm. The tensile tests were conducted at room temperature at the crosshead speed of 0.5 mm·min^{-1} by CMT5105 tensile testing machine. The mechanical properties of the joint were measured and the average value of three tensile specimens cut from the same weld plate was used. The Vickers hardness of cross-section of the polished specimen was measured at the load of 0.98 N and dwell time of 15 s. The microstructure characteristics and element distributions along the interface were analyzed by scanning electron microscope (SEM) equipped with energy dispersive X-ray spectroscope (EDS). In order to obtain the temperature and strain distributions along the joint, the ABAQUS software was used to build the thermal-mechanical coupled model of FSW process based on the coupled Eulerian-Lagrangian (CEL) model.

2 Results and Discussion

2.1 Microstructure

The cross-section microstructures and EDS analyses of bonding interface of 6061Al/QP980 steel joint after friction stir lap-welding with short and long probes are shown in Fig.2 and Fig. 3, respectively. As shown in Fig. 2, the stir zone is only in Al alloy side. Whereas for the joints welded by the long probe, the stir zone expands to steel side (Fig. 3). The cross-section morphologies also reveal that the lap-welded joints have good surface quality at the stir zone and neighboring areas.

It can be seen from Fig.2 that the lap-welded joint prepared by short probe consists of three layers: the stir zone of 6061Al alloy, IMC layer, and QP980 steel. Similarly, three distinct regions can also be observed in the lap-welded joints prepared by long probe: the top layer consisting of 6061Al matrix with scattered steel fragments, the middle layer consisting of Fe-Al solid solutions of lamellar structure with IMCs, and the bottom steel layer with stir zone. The scattered steel fragments inside the Al matrix are surrounded by IMC layer. It is known that the IMCs are generally formed along the Al/Fe interface due to the high temperature which promotes the element

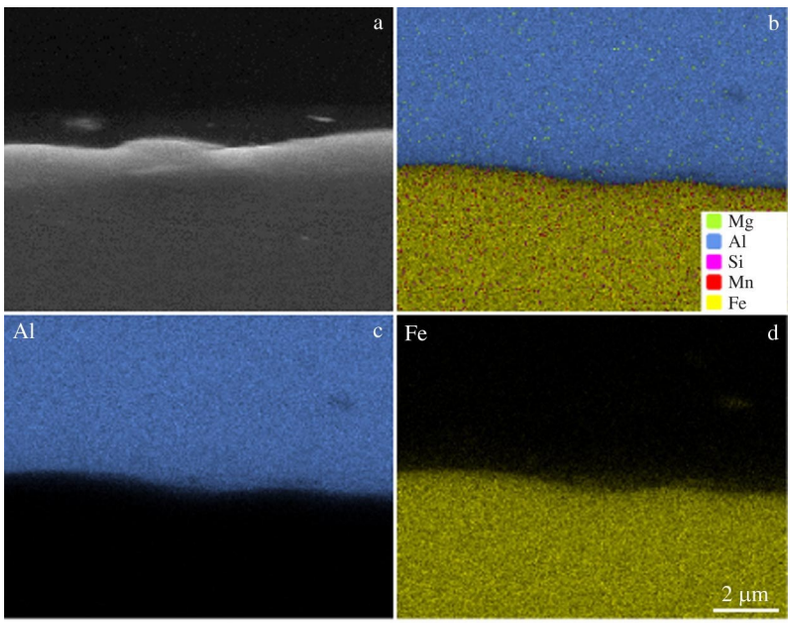

Fig.2 Cross-section microstructure (a) and EDS element distributions (b~d) of bonding interface of 6061Al/QP980 steel joint after friction stir lap-welding with the short probe: (b) overall element distribution; (c) Al distribution; (d) Fe distribution

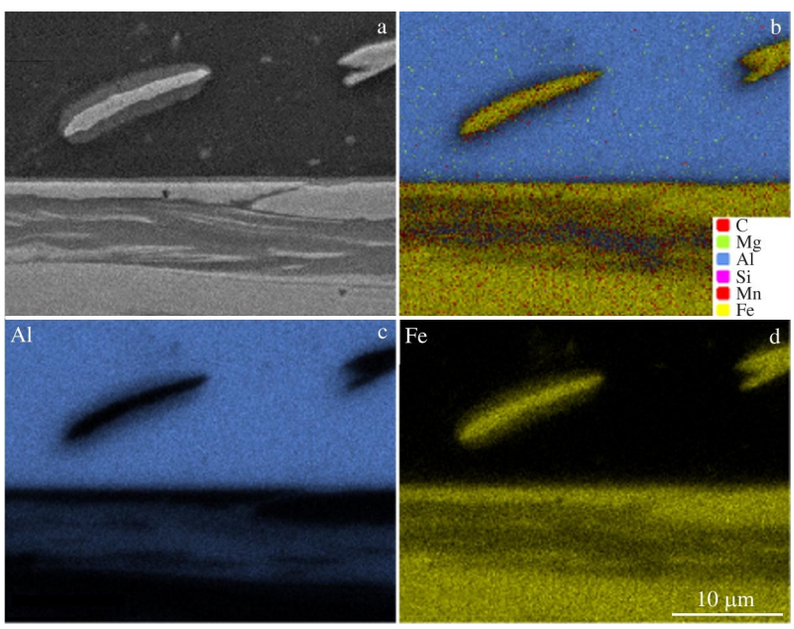

Fig.3 Cross-section microstructure (a) and EDS element distributions (b~d) of bonding interface of 6061Al/QP980 steel joint after friction stir lap-welding with the long probe: (b) overall element distribution; (c) Al distribution; (d) Fe distribution

mutual diffusions during the welding process[22].

The variations of Al and Fe elements across the bonding interface of the stir zone are analyzed through the arrow marked in Fig. 4a. It is clear that the Al content is decreased while the Fe content is increased along the arrow from 6061Al side to QP980 steel side. Two kinds of IMCs can be observed. Four points S1~S4 are chosen for phase component analysis, and EDS analysis results are shown in Table 3. It can be speculated that the dark grey layer (S2) close to Al matrix is Fe_4Al_{13} phase, and the bright grey layer (S3) close to steel matrix is Fe_2Al_5 phase.

The temperature distributions at different layers of the joint cross-section (displacement=0 μm) perpendicular to the tool transverse direction are predicted by the thermal-mechanical coupled model, as shown in Fig. 5a and 5b. The peak temperature of 510 °C is obtained at the 6061Al matrix side for the lap-welded joint prepared by short probe, because the 6061Al matrix has direct contact with the tool shoulder, thereby generating most heat during FSW process. This temperature is about 90% of the melting point of 6061Al alloy

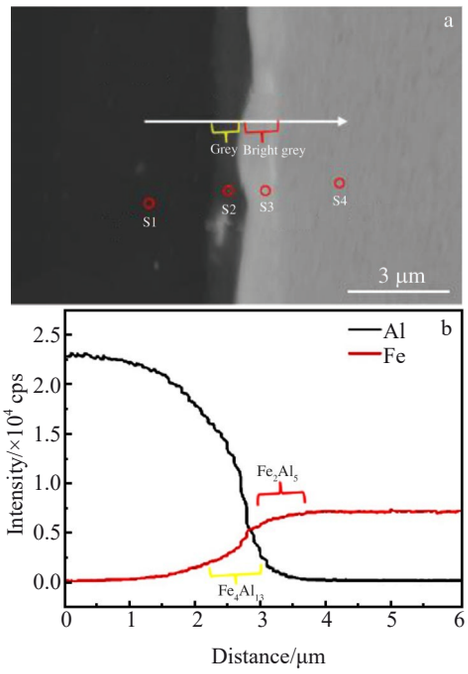

Fig.4 Cross-section microstructure (a) and element distributions along the white arrow marked in Fig. 4a (b) in bonding interface

and only plastic deformation occurs in the joints during welding process. Therefore, no casting-induced voids or cracks are formed in the joint microstructure, as shown in Fig.6a. The peak temperature is 640 °C at QP980 steel side for the lap-welded joint prepared by long probe (Fig.5b), which is higher than that prepared by short probe. This phenomenon is related to the difference in specific heat capacity of Al (0.88 $kJ \cdot kg^{-1} \cdot K^{-1}$) and steel (0.46 $kJ \cdot kg^{-1} \cdot K^{-1}$) and the probe rotation in steel. It can be concluded that the sufficient heat is generated to soften the material. The high temperature leads to the melted Al, and thus the microstructure with voids and cracks can be observed in Fig. 6b. The formation of void defect can be explained by the stirring of the liquid phase (Al alloy) with low melting point in the stir zone resulting from the synthetic effect of high temperature and deformation caused by the application of long probe. The results indicate that the short probe is beneficial to obtain lap-welded Al/steel joints. The strain distributions across the bonding interface of the joints predicted by thermal-mechanical coupled model are presented in Fig. 5c and 5d. The longer the probe length, the higher the strain. In addition, the highest strain is achieved at the 6061Al matrix side because of the stirring of the shoulder and probe.

Table 3 EDS analysis results of S1~S4 points in Fig.4a (at%)

Point	Mg	Al	Si	Mn	Fe	Phase
S1	3.38	95.60	0.26	0.10	0.66	α-Al
S2	1.77	78.25	0.86	0.48	18.65	Fe_4Al_{13}
S3	2.50	65.56	1.81	0.75	29.32	Fe_2Al_5
S4	0.47	18.98	2.57	1.93	76.05	γ-Fe

Due to the thermo-mechanical influence of FSW tool on the weld regions, the microstructure refinement in welded joints occurs due to the recrystallization caused by strain and temperature[23]. In this research, the 6061Al/QP980 steel joint is subjected to high temperature (510~640 ° C) and large

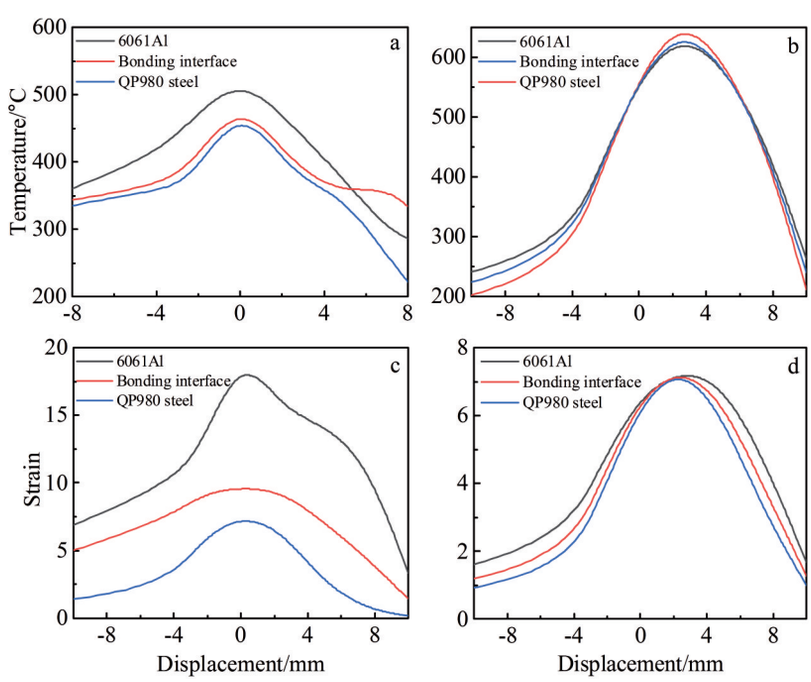

Fig.5 Temperature (a, b) and strain (c, d) distributions of 6061Al/QP980 steel joint after friction stir lap-welding with short (a, c) and long (b, d) probes

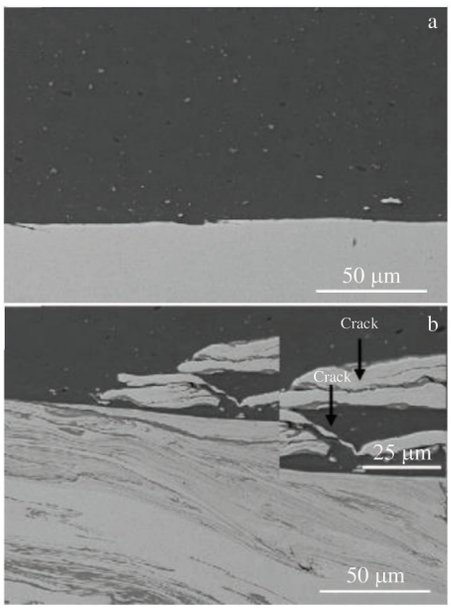

Fig.6 SEM microstructures of 6061Al/QP980 steel joint after friction stir lap-welding with short (a) and long (b) probes

deformation (effective strain of 10~18) during FSW process, which results in dynamic recrystallization in aluminum alloy. The continuous dynamic recrystallization occurs in 6061Al/QP980 steel joint during FSW due to the high stacking fault energy[24,25]. Fig. 7 shows the grain orientations in different positions of 6061Al/QP980 steel joint. At the 6061Al side, the obviously refined grains can be observed. The average grain sizes in stir zones of 6061Al and QP980 steel matrixes are 6.25 and 5.10 μm, respectively, which are much smaller than those of the original materials.

2.2 Mechanical properties

The Vickers hardness of 6061Al/QP980 steel joints after friction stir lap-welding with short and long probes is shown in Fig. 8. The distance between adjacent measured points is 0.5~1 mm. The hardness $HV_{0.1}$ of original 6061Al alloy is 637~686 MPa. However, the hardness $HV_{0.1}$ of the stir zone in the joint prepared by either the long or the short probe is reduced to 588~637 MPa. This reduction is mainly attributed to the associated thermal cycles caused by the friction between shoulder and welded plates, which exerts the annealing effect essentially. During the thermal cycles, the grains and strengthened phases are coarsened, which weakens

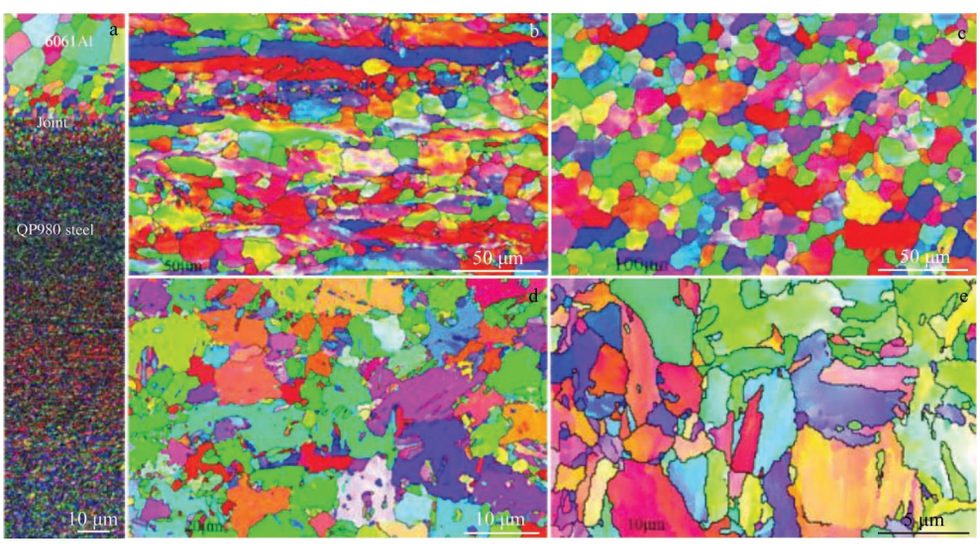

Fig.7 Grain orientations of cross-section of 6061Al/QP980 steel joint (a), 6061Al matrix (b), stir zone of 6061Al matrix (c), QP980 steel matrix (d), and stir zone of QP980 steel matrix (e)

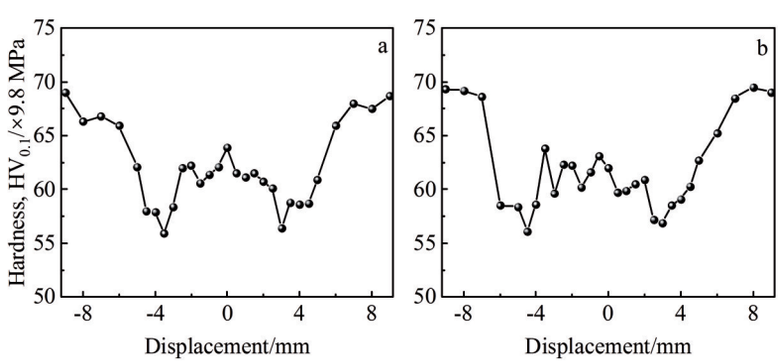

Fig.8 Vickers hardness $HV_{0.1}$ of 6061Al/QP980 steel joint after friction stir lap-welding with short (a) and long (b) probes

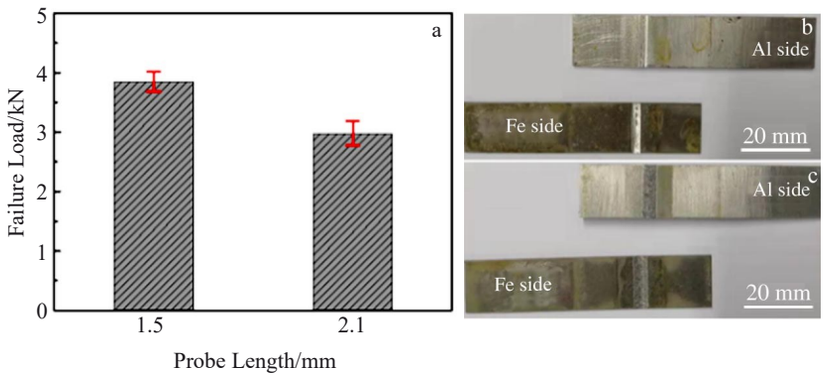

Fig.9 Tensile strength of 6061Al/QP980 steel joints after friction stir lap-welding (a); appearances of fracture locations of 6061Al/QP980 steel joints after friction stir lap-welding with short (b) and long (c) probes

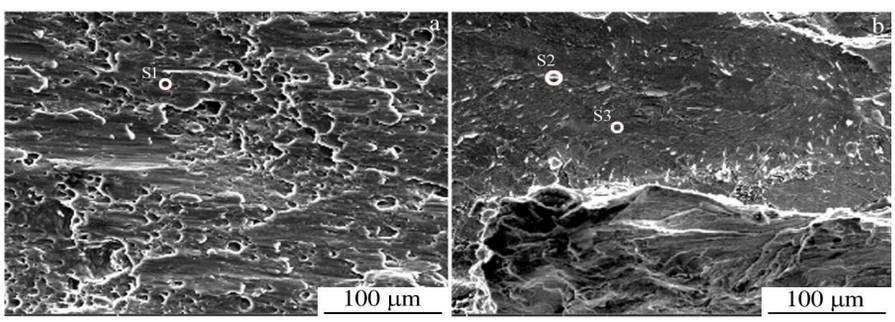

Fig.10 SEM fracture morphologies of 6061Al/QP980 steel joints after friction stir lap-welding with short (a) and long (b) probes

the strengthening effect. The further the distance from the heat-affected zone, the higher the hardness in the joint. In addition, the hardness of welded joints prepared by long probe shows a larger fluctuation due to the nonuniform microstructure caused by high temperature and detached fragments of steel.

Fig. 9 shows the effect of probe length on the tensile strength and fracture locations of lap-welded 6061Al/QP980 steel joints. The fracture loads for the joints prepared by short and long probes are ~4 and ~3 kN, respectively. Thus, the better tensile strength is obtained for the joints prepared by short probe. The materials in the interface region undergo synthetic effect of thermal cycles and the mechanical cycles during FSW process, thereby resulting in the microstructure evolution and fracture behavior of the welded parts. For the joints prepared by short probe, the thermal cycle accelerates the mutual diffusion of Al and Fe atoms. As a result, the metallurgical bonding forms and the joints are strengthened. However, the fracture load of the joints prepared by long probe is relatively low. When the probe penetrates the QP980 steel, a large number of steel fragments are distributed in the bonding interface and even into the 6061Al matrix. Besides, the void defects exist in the joint due to the melt of aluminum alloy. These steel fragments and void defects are the suitable sites for crack initiation and propagation during tensile tests[26]. It can be seen from Fig. 9 that the joints prepared by short probe fracture at the bonding interface of 6061Al matrix side (Fig. 9b), whereas the fracture occurs at the stir zone of bonding interface in joints prepared by long probe (Fig. 9c). The weakest part of the joints changes from the bonding interface to the stir zone of 6061Al side with decreasing the probe length, which is consistent with the change of mechanical properties.

SEM fracture morphologies of 6061Al/QP980 steel joints after tensile tests are shown in Fig. 10. For the joints prepared by short probe, the cleavage steps and partial dimples can be observed in Fig. 10a, indicating that the fracture mode is ductile-brittle fracture. For the joints prepared by long probe, the cleavage steps, river patterns, tear ridges, and some micro-voids appear on the fracture surface, as shown in Fig. 10b, suggesting the quasi-cleavage brittle fracture. In addition, according to Table 4, some brittle Fe-rich IMCs are embedded in the fracture surface of 6061Al matrix in the joint prepared by short probe. Based on the results of S2 and S3 points in Table 4, the fracture is related to brittle secondary phases, which are the stress concentration locations for the joints prepared by long probe.

Table 4 Element contents at fracture positions in Fig. 10 of 6061Al/QP980 steel joints after friction stir lap-welding (at%)

Position	Mg	Al	Si	Mn	Fe
S1	3.18	96.82	-	-	-
S2	1.71	66.88	1.08	1.01	29.33
S3	-	52.37	-	1.52	46.11

3 Conclusions

1) The 6061Al/QP980 steel joints prepared by friction stir lap-welding with short probe do not contain flaws, voids, nor cracks, and they fracture at the stir zone of 6061Al matrix side. The higher fracture load is obtained and the fracture mode is the mixed ductile-brittle fracture for the joints prepared by short probe.

2) The steel fragments are distributed in the bonding interface and even in the 6061Al matrix during the lap-welding of joints with long probe. Meanwhile, the voids and cracks are formed due to the high temperature and steel fragments. Thus, the fracture load is relatively low and the fracture mode is quasi-cleavage brittle fracture.

3) The bonding interface region undergoes the synthetic effect of the thermal cycles (510~640 °C) and the mechanical cycles (strain of 10~18) during friction stir lap-welding process, because of the friction, stir, and extrusion of the shoulder and probe. The Fe_4Al_{13} phase is formed close to 6061Al matrix and the Fe_2Al_5 phase is formed close to QP980 steel matrix.

References

1 Zhou L, Yu M R, Liu B Y *et al. Journal of Materials Research and Technology*[J], 2020, 9(1): 212

2 Wei Y N, Li J L, Xiong J T *et al. Materials & Design*[J], 2012, 33: 111

3 Cao R, Sun J H, Chen J H *et al. Welding Journal*[J], 2014, 93: 193

4 Lu Y, Sage D D, Fink C *et al. Science and Technology of Welding and Joining*[J], 2020, 25(3): 218

5 Peng Y Y, Yin Z M, Lei X F *et al. Rare Metal Materials and Engineering*[J], 2011, 40(2): 201

6 Luo J, Chen W, Fu G. *Journal of Materials Processing Technology*[J], 2014, 214(12): 3002

7 Singh K, Singh G, Singh H. *Journal of Magnesium and Alloys*[J] 2018, 6(4): 399

8 Lin H T, Jiang H T, Wang Y S *et al. Materials Research Express* [J], 2019, 12(6): 126 584

9 Ramachandran K K, Murugan N, Kumar S S. *Welding Journal* [J], 2015, 94: 291

10 Kasai H, Morisada Y, Fujii H. *Materials Science and Engineering A*[J], 2015, 624: 250

11 Rodrigues D M, Loureiro A, Leitao C *et al. Materials & Design* [J], 2009, 30(6): 1913

12 Vysotskiy I, Malopheyev S, Rahimi S *et al. Materials Science and Engineering A*[J], 2019, 760: 277

13 Yazdipour A, Heidarzadeh A. *Journal of Alloys and Compounds* [J], 2016, 680: 595

14 Moraes J F C, Rodriguez R I, Jordon J B *et al. International Journal of Fatigue*[J], 2017, 100: 1

15 Zhang C, Huang G, Cao Y *et al. Materials Science and Engineering A*[J], 2019, 766: 138 368

16 Pourali M, Abdollah-Zadeh A, Saeid T *et al. Journal of Alloys and Compounds*[J], 2017, 715: 1

17 Zhao S, Ni J, Wang G Q *et al. Journal of Materials Processing Technology*[J], 2018, 261: 39

18 Dehghani M, Amadeh A, Mousav S A A. *Materials & Design*[J], 2013, 49: 433

19 Bozzi S, Helbert-Etter A L, Baudin T *et al. Materials Science and Engineering A*[J], 2010, 527(16-17): 4505

20 Chen Y C, Komazaki T, Kim Y G *et al. Materials Chemistry and Physics*[J], 2008, 111(2): 375

21 Chen Y C, Nakata K. *Materials & Design*[J], 2019, 30(9): 3913

22 Abbasi M, Dehghani M, Guim H U *et al. Acta Materialia*[J], 2016, 117: 262

23 Kumar A V, Balasrinivasan M, Kumar R V *et al. Materials Today: Proceedings*[J], 2020, 22: 1333

24 Miles M P, Nelson T W, Gunter C *et al. Journal of Materials Science & Technology*[J], 2019, 35(4): 491

25 Yang C L, Wu C S, Shi L. *Science and Technology of Welding and Joining*[J], 2020, 25(4): 345

26 Mahto R P, Kumar R, Pal S K. *Materials Characterization*[J], 2020, 160: 110 115

搅拌针长度对搅拌摩擦搭接焊铝合金/钢异种材料接头组织性能的影响

武晓燕，罗　巍，江海涛

(北京科技大学 高效轧制与智能制造国家工程研究中心，北京 100083)

摘　要：通过搅拌摩擦搭接焊接6061铝合金/QP980钢异种材料，讨论了搅拌针长度（1.5和2.1 mm）对焊接接头组织和性能的影响。结果表明，6061铝合金/QP980钢搅拌摩擦搭接焊接头分为3层结构：上层为铝合金层，中间层为Fe、Al及金属间化合物混合层状结构，下层为钢层。其中，当搅拌针长2.1 mm时，铝合金层含有散落的钢碎片。在中间层检测到2种金属间化合物，靠近Al的深灰色层为Fe_4Al_{13}相，靠近钢的是Fe_2Al_5相。随着搅拌针长度的增加，接头的失效载荷从4 kN降低到3 kN。短探针焊接的接头在接合界面处断裂，而长探针焊接的接头在铝和钢的混合区断裂。孔洞缺陷和钢碎片是导致断裂位置发生变化的主要原因。此外，嵌入铝基体中的铁屑在变形过程中起应力集中和裂纹萌生的作用，降低了接头的力学性能。

关键词：搅拌摩擦搭接焊；搅拌针长度；金属间化合物；失效载荷

作者简介：武晓燕，女，1989年生，博士，北京科技大学高效轧制与智能制造国家工程研究中心，北京 100083，电话：010-62332598，E-mail：wuxiaoyan@ustb.edu.cn